



Verification of competitive kinetics technique and oxidation kinetics of 2,6-dimethyl-aniline and *o*-toluidine by Fenton process

Jin Anotai^{a,*}, Nacorn Panchanawaporn^a, Nonglak Boonrattanakij^{b,c}, Ming-Chun Lu^d

^a National Center of Excellence for Environmental and Hazardous Waste Management, Department of Environmental Engineering, Faculty of Engineering, King Mongkut's University of Technology Thonburi, Pracha-u-tid Road, Bangmod, Thungkru, Bangkok 10140, Thailand

^b International Postgraduate Programs in Environmental Management, Graduate School, Chulalongkorn University, Bangkok 10330, Thailand

^c National Center of Excellence for Environmental and Hazardous Waste Management (NCE-EHWM), Chulalongkorn University, Bangkok 10330, Thailand

^d Department of Environmental Resources Management, Chia-Nan University of Pharmacy and Science, Tainan 717, Taiwan

ARTICLE INFO

Article history:

Received 28 December 2010

Accepted 25 January 2011

Available online 1 February 2011

Keywords:

Advanced oxidation processes

Fluidized-bed Fenton

Hydroxyl radicals

Mechanism

ABSTRACT

The competitive kinetics technique is shown to be a useful and reliable tool for determining rate constants. Regardless of the conditions of the reaction and the operation mode, the intrinsic second-order rate constants of 2,6-dimethyl-aniline and hydroxyl radicals were 1.65×10^{10} , 1.60×10^{10} , and $1.71 \times 10^{10} \text{ M}^{-1} \text{ s}^{-1}$ in the absence of SiO_2 under complete-mix conditions, in the presence of SiO_2 under complete-mix conditions, and in a fluidized-bed Fenton reactor with SiO_2 as the media, respectively, demonstrating that the rates are comparable under a variety of reaction conditions. The average intrinsic second-order rate constant of *o*-toluidine and hydroxyl radicals obtained in a homogeneous system under various conditions was $7.36 \times 10^9 \text{ M}^{-1} \text{ s}^{-1}$, indicating that *o*-toluidine is less susceptible to hydroxyl radicals than 2,6-dimethyl-aniline. Hydroxyl radicals primarily attacked the amine group rather than the methyl group of the *o*-toluidine to form *o*-cresol and 2-nitrotoluene, which sequentially transformed to carboxylic acids including acetic, oxalic, lactic, and maleic acids after the collapse of the benzene ring.

© 2011 Elsevier B.V. All rights reserved.

1. Introduction

o-Toluidine (OT) is used in many factories to produce products such as dyestuffs, pharmaceuticals, pesticides, and antioxidants [1]. This chemical is considered to possibly be carcinogenic to humans according to the International Agency for Research on Cancer [2]. Therefore, it must be removed from wastewater before discharge into the environment. Ordinary biological processes are neither suitable nor effective for removing OT [3,4]. Other advanced treatment alternatives, including chemical and physicochemical processes, must be considered. Advanced oxidation processes (AOPs) represent one chemical approach that has been found to very effectively remove refractory organic pollutants in water and air. AOPs generate a sufficient amount of the hydroxyl radical (OH^\bullet), which is a very powerful and non-selective oxidant that can effectively oxidize and/or mineralize a wide range of organic compounds including recalcitrant pollutants [5]. The Fenton process is a type of AOP that does not require sophisticated or expensive equipment but still very effectively generates

OH^\bullet . However, the intrinsic rate constant between OT and OH^\bullet has not been reported [6] and deserves investigation. OH^\bullet is a transient species, and direct assessment of its trace concentration is possible but impractical. As a result, the ordinary approach for determining a rate constant is not feasible in this case. To overcome this burden, the competitive kinetics technique in which a reference compound with a known rate constant coexists in the homogeneous solution during the reaction period was used to determine the rate constant of the target compound and OH^\bullet [7,8]. It was the aim of this study to determine the accuracy of this competitive kinetics technique under various conditions, particularly homogeneous versus heterogeneous and complete mix versus fluidized-bed conditions. Thus, the first objective of this study was to determine the rate constant of 2,6-dimethyl-aniline (2,6-DMA), another hazardous compound [9], in OH^\bullet oxidation under heterogeneous conditions and compare the result to the rate constant obtained under homogeneous conditions. The second objective was to apply the competitive kinetic technique to determine the intrinsic rate constant and mechanism of the reaction between OT and OH^\bullet in the Fenton process which have not been previously reported. Aniline (AN) was selected as a reference compound in this study because its molecular structure is quite similar to OT and 2,6-DMA and can accurately quantified under the same gas chromatography conditions.

* Corresponding author. Tel.: +66 2 470 9166; fax: +66 2 470 9165.

E-mail address: jin.ano@kmutt.ac.th (J. Anotai).

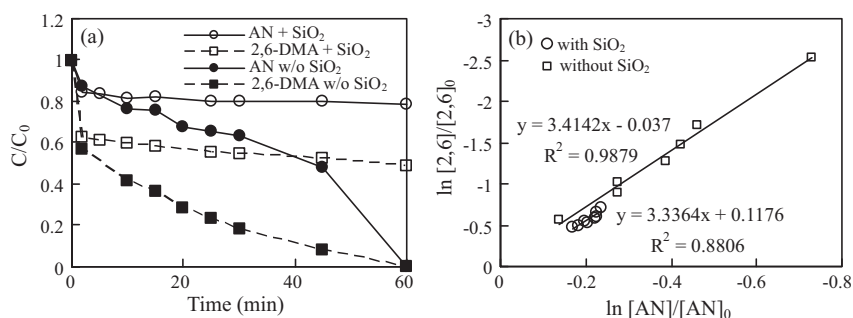


Fig. 1. Effect of SiO_2 on organic oxidation and rate constant in the experiment with 1 mM of AN, 1 mM of 2,6-DMA, 1 mM of Fe^{2+} , 20 mM of H_2O_2 , 37.04 g/l of SiO_2 at pH 3 and 25 °C: (a) profile of AN and OT oxidation and (b) plot of Eq. (3).

2. Materials and methods

2.1. Materials and reagents

o-Toluidine, 2,6-DMA, AN, ferrous sulfate ($\text{FeSO}_4 \cdot 7\text{H}_2\text{O}$), hydrogen peroxide (H_2O_2), sulfuric acid (H_2SO_4), and sodium hydroxide (NaOH) were reagent-grade. Demineralized water from the Millipore System with a resistivity of $18.2 \text{ M}\Omega \text{ cm}^{-1}$ was used to prepare all solutions. Silica dioxide (SiO_2) particles with sizes between 0.42 and 0.59 μm (passing sieve #30 and retained on sieve #40) were used as the suspended/fluidized media in the heterogeneous Fenton study. The SiO_2 was soaked in HCl solution at pH 1 for 24 h, rinsed with deionized water until the pH of the rinse water was 7, and then oven-dried at 103 °C before use.

2.2. Experimental setup

To verify the competitive kinetics technique, the Fenton reaction was carried out under two sets of conditions, i.e., the homogeneous and heterogeneous modes. In the heterogeneous study, SiO_2 was used as a media under two sets of working conditions: complete-mix and fluidized-bed configurations. In the complete-mix experiment, the synthetic wastewater was prepared in a 0.5-liter Pyrex beaker by dissolving appropriate amounts of 2,6-DMA with AN and $\text{FeSO}_4 \cdot 7\text{H}_2\text{O}$. SiO_2 was also added to the solution in the heterogeneous study. The solution/mixture was then adjusted to pH 3 by adding either H_2SO_4 or NaOH. Finally, the H_2O_2 was added and the Fenton reaction began. The fluidized-bed Fenton experiment employed a glass cylinder 5.23 cm in diameter and 133 cm in height with internal recirculation similar to that used in the study of Anotai et al. [10]. The SiO_2 bed was constantly expanded at 50% of its original volume by adjusting the internal recirculation rate. For the OT kinetics study, the experimental setup was similar to the setups of the 2,6-DMA kinetics studies in the completely mixed reactor, except OT was used instead of 2,6-DMA and SiO_2 was not present. All experiments were conducted in batch

mode. The reactor was controlled at $\text{pH } 3.0 \pm 0.05$ and 25 ± 0.5 °C throughout the experimental period. Samples were taken at predetermined times, filtered through 0.22 μm filter paper, and injected into a sodium hydroxide solution to prevent any further Fenton reaction. The mixture was filtered again to remove precipitated iron before beginning the analysis for organic compounds and oxidation intermediates. Fe^{2+} and H_2O_2 were monitored throughout the experiment to ensure the continuity of the Fenton reaction. A filtered sample without alkaline treatment was used to determine the residual Fe^{2+} and H_2O_2 , and the analyses were performed immediately after sampling.

2.3. Analytical methods

Residual organic compounds were analyzed by a Shimadzu GC-17A gas chromatograph (Japan) equipped with a flame ionization detector and a Hewlett-Packard HP-5 capillary column (USA) 0.53 mm in diameter and 15 m in length. 1 μL of each sample was injected into the injection port. The temperature of the column was initially set to 85 °C and equilibrated for 3 min. The column temperature was then raised to 200 °C at a ramp rate of 65 °C min^{-1} and maintained at 200 °C for 5 min. The injector and detector temperatures were set to 250 °C. The ferrous content was determined using the phenanthroline method detailed in Standard Methods [11]. The residual H_2O_2 content was analyzed by iodometric titration with $\text{Na}_2\text{S}_2\text{O}_3$ solution [12]. The solution pH was measured by a Bantex Portable pH-1000 Meter (Taiwan). For identification of aromatic intermediates, 1.0 μL of the extracted solvent was injected into an Agilent Technologies 6890N Network GC System (USA) equipped with a J&W DB-5MS capillary column (USA) 0.25 mm in diameter and 30 m in length and connected to a 5973 Network Mass Selective Detector (USA). The GC temperature was initially set to 40 °C for 2 min, ramped to 280 °C at 15 °C min^{-1} , then held at 280 °C for 5 min. The carboxylic acid content was determined by a Shimadzu Ion Chromatograph System (Japan) equipped with a SCL-10AVP system

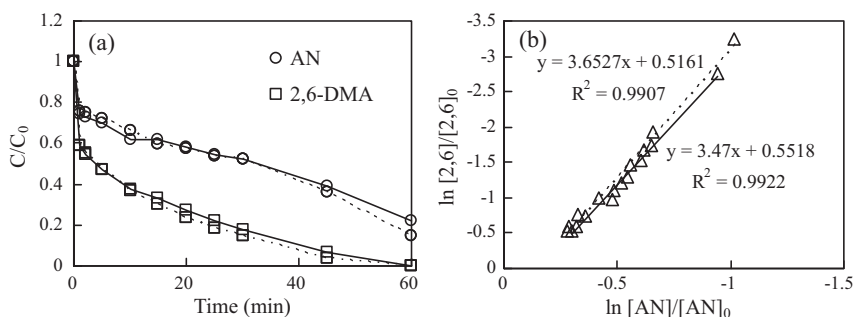


Fig. 2. Organic oxidation and rate constant determination in the fluidized-bed Fenton reactor with 1 mM of AN, 1 mM of 2,6-DMA, 1 mM of Fe^{2+} , 20 mM of H_2O_2 , 230.77 g/l of SiO_2 , pH 3 and 25 °C: (a) profile of AN and OT oxidation and (b) plot of Eq. (3) (solid line is run #1 and dotted line is run #2).

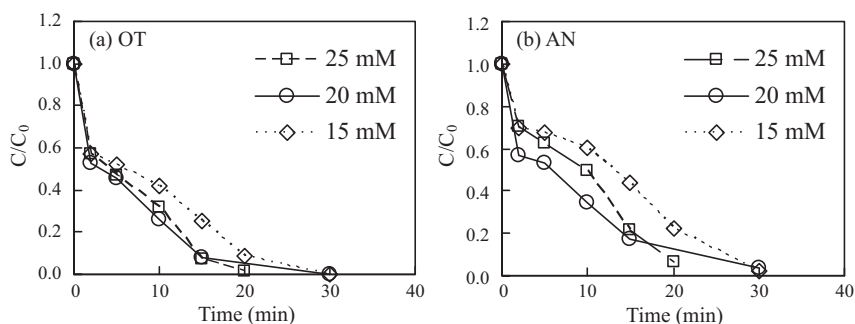


Fig. 3. Effect of H_2O_2 on the oxidation of AN and OT under the following conditions: 1 mM of AN, 1 mM of OT, 1 mM of Fe^{2+} at pH 3 and $25^\circ C$.

controller, DGU-20A3 degasser, LC-20ADVP liquid chromatograph, CTO-20A column oven, CDD-20ASP conductivity detector, SIL-10Ai auto injector, Shim-pack IC-GA3 guard column, and Shim-pack IC-A3 analytical column (4.6 mm \times 15 cm). The mobile phase was 3.2 mM bis(2-hydroxyethyl)iminotris(hydroxymethyl)methane and 8.0 mM *p*-hydroxybenzoic acid. The flow rate and temperature were set to 1.2 mL min^{-1} and $40^\circ C$, respectively. The injected sample volume was 10 μL .

3. Results and discussion

3.1. Control experiments

The effects of direct H_2O_2 oxidation, ferric coagulation (after alkali termination of Fenton reaction), and volatilization on the OT, 2,6-DMA, and AN concentrations in aqueous phase must be determined. The results showed that none of these organic compounds could be significantly removed without the Fenton reaction, i.e., H_2O_2 oxidation, volatilization, and adsorption onto ferric hydroxide precipitates provided less than 5% reduction in all cases. As a result, the disappearance of these compounds during the experiment should come only from OH^\bullet oxidation.

3.2. Verification of the competitive-rate technique

This portion of the experiment was conducted to determine the effect of the presence of solid particles during the reaction on the accuracy of the competitive kinetics technique. Oxidation of OH^\bullet with any pollutant can be described as a second-order reaction with respect to the OH^\bullet and pollutant concentrations. For a batch reactor such as the one used in this study, the competitive rate equations for OH^\bullet oxidation in the presence of two organic pollutants (P_1 and P_2) can be written as shown in Eqs. (1) and (2) and can be further manipulated to obtain a final relationship that does not include the

OH^\bullet concentration in Eq. (3) [7,8].

$$\frac{d[P_1]}{dt} = -k_{p_1}[P_1][OH^\bullet] \quad (1)$$

$$\frac{d[P_2]}{dt} = -k_{p_2}[P_2][OH^\bullet] \quad (2)$$

$$\ln \left(\frac{[P_1]_t}{[P_1]_0} \right) = \frac{k_{p_1}}{k_{p_2}} \ln \left(\frac{[P_2]_t}{[P_2]_0} \right) \quad (3)$$

where $[P_1]_0$, $[P_1]_t$, and $[P_2]_0$, $[P_2]_t$ are the concentrations of P_1 and P_2 at the time 0 and time "t", respectively; $[OH^\bullet]$ is the concentration of OH^\bullet ; k_{p_1} and k_{p_2} are the reaction rate constants of OH^\bullet with P_1 and P_2 , respectively. Since $[P_1]_0$, $[P_1]_t$, $[P_2]_0$ and $[P_2]_t$ can be measured and k_{p_2} of the reference compound is known, the k_{p_1} of the target compound can be determined.

In the first test, SiO_2 was suspended in a batch Fenton reactor under complete-mix conditions to simulate a heterogeneous environment. The rate constant of 2,6-DMA with OH^\bullet was investigated and compared to the values obtained from the homogeneous system in the absence of SiO_2 . It was found that the presence of SiO_2 deteriorated the overall oxidation rate of 2,6-DMA, as shown in Fig. 1(a). This may be due to limitation of Fe^{2+} in the presence of the SiO_2 suspension resulting from surface complexation. A certain fraction of the added Fe^{2+} was adsorbed onto SiO_2 surfaces, reducing the amount of free Fe^{2+} available to catalyze the decomposition of H_2O_2 and generate the powerful OH^\bullet . As a result, the disappearance rates of aniline and 2,6-DMA decelerated. Nonetheless, the results showed that the ratio between the rate constants of 2,6-DMA and AN with OH^\bullet , which are represented by the slopes in the plot of Eq. (3) in Fig. 1(b), were comparable in the absence and presence of the SiO_2 suspension (3.4142 versus 3.3364). From the known rate constant between AN and OH^\bullet ($4.8 \times 10^9 \text{ M}^{-1} \text{ s}^{-1}$ from Buxton et al. [6]), the rate constants between 2,6-DMA and OH^\bullet were found to be 1.64×10^{10} and $1.60 \times 10^{10} \text{ M}^{-1} \text{ s}^{-1}$ in the absence and presence of SiO_2 , respectively. These values were very close to the value of $1.71 \times 10^{10} \text{ M}^{-1} \text{ s}^{-1}$ reported by Boonrattanakij

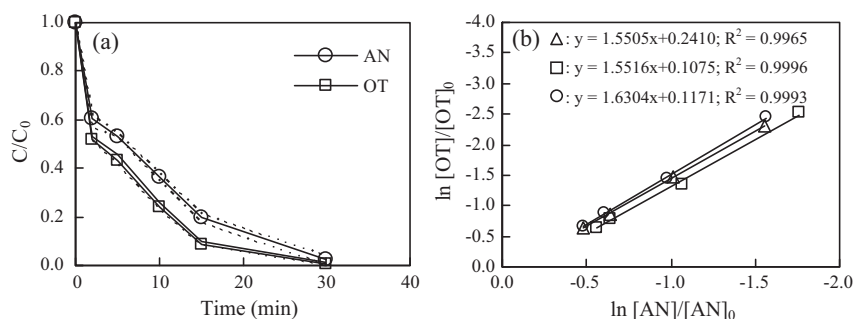


Fig. 4. Rate constant determination for the experiments with 1 mM of AN, 1 mM of OT, 1 mM of Fe^{2+} , 20 mM of H_2O_2 at pH 3 and $25^\circ C$: (a) profile of AN and OT oxidation, dotted lines represent the upper and lower bounds and (b) plot of Eq. (3).

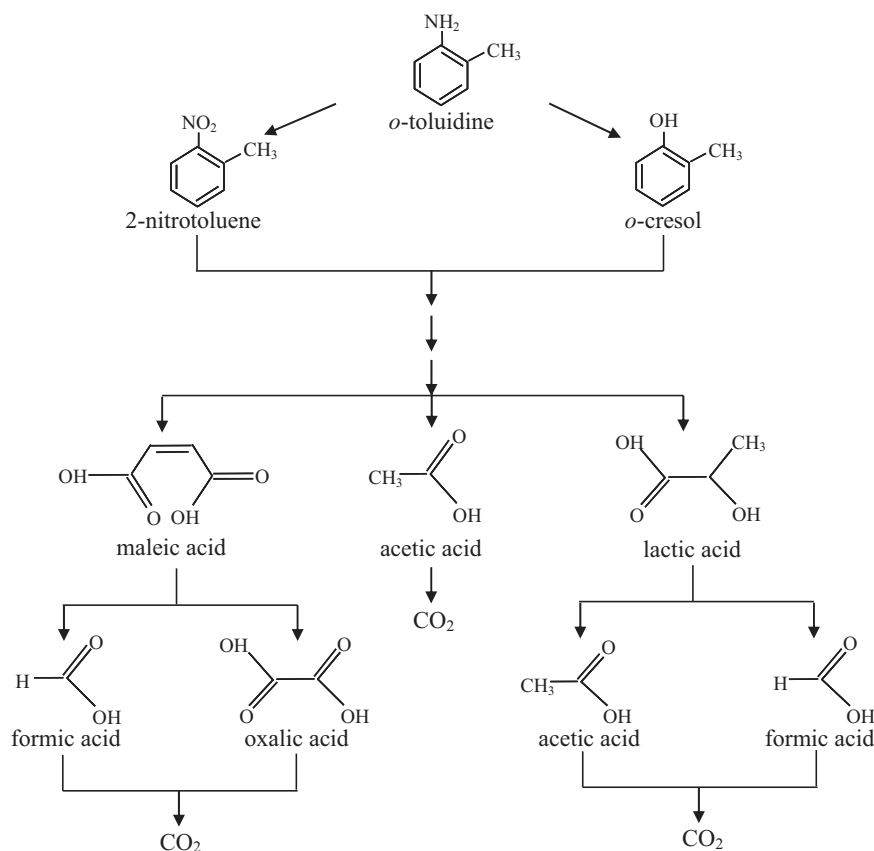


Fig. 5. Proposed reaction pathway for *o*-toluidine oxidation by hydroxyl radicals.

et al. [8] who used a homogeneous Fenton reactor. Thus, the competitive kinetics technique is shown to be effective and accurate. To confirm this result, two other experiments were conducted in a fluidized-bed Fenton reactor operated in batch mode using SiO₂ as the fluidized media. It can be seen in Fig. 2(a) that the data obtained in two different runs with similar conditions were nearly the same, verifying the consistency of the experimental setup and procedure. The average slope was 3.5614 (Fig. 2(b)), which corresponds to a rate constant of $1.71 \times 10^{10} \text{ M}^{-1} \text{ s}^{-1}$. This value is in the proximity of the values obtained in the complete-mix study and the value reported by Boonrattanakij et al. [8]. As a result, it can be firmly concluded that the competitive kinetics technique is a useful and reliable tool for rate constant determination regardless of the system configuration and the conditions of the reaction.

3.3. Kinetics characterization of *o*-toluidine oxidation by hydroxyl radicals

3.3.1. Effect of Fe²⁺-H₂O₂ ratio

It is well documented that Fenton's reagent, Fe²⁺ and H₂O₂, not only produces OH• but also scavenges the generated OH• if it is present in an excessive amount. As a result, too much Fenton's reagent can deteriorate the performance of the Fenton reaction. This part of the experiment aimed to determine the Fe²⁺:H₂O₂ molar ratio that optimizes the organic degradation under the studied conditions. The optimum ratio was found to be around 1:20, as shown in Fig. 3, i.e., the organic oxidation performance decreased when the amount of H₂O₂ was higher or lower than the noted optimum concentration. Nonetheless, it is important to note that the Fe²⁺:H₂O₂ molar ratio will not interfere with the accuracy of determining the rate constant using the competitive kinetics technique, as the target and reference com-

pounds are both exposed to the same OH• concentration at all times.

3.3.2. Intrinsic rate constant determination

Fig. 4 is an example plot of the determination of the rate constant between OT and OH• under homogeneous conditions. This experiment was performed in triplicate, and the data from each repetition were very similar, assuring the repeatability and accuracy of the experimental procedure. The slopes in Fig. 4(b) represents the ratio of the rate constants between OT and AN, indicating that OT reacts with OH• 1.55–1.63 times more rapidly than AN, which is still slower than 2,6-DMA. This is reasonable as the oxidation state of carbon atoms in 2,6-DMA is lower than that in either OT or AN. Hence, the OH• favorably attacks 2,6-DMA, followed by OT and finally AN. Table 1 summarizes all of the rate constants obtained

Table 1
Intrinsic 2nd-order rate constants between *o*-toluidine and hydroxyl radicals.

Run no.	AN (mM)	OT (mM)	Fe ²⁺ (mM)	H ₂ O ₂ (mM)	<i>k</i> (M ⁻¹ s ⁻¹)
1	1	1	1.0	15	7.70×10^9
2	1	1	1.0	20	7.44×10^9
3	1	1	1.0	20	7.45×10^9
4	1	1	1.0	20	7.83×10^9
5	1	1	1.0	25	7.32×10^9
6	2	2	1.0	20	7.58×10^9
7	2	2	1.0	20	7.54×10^9
8	2	2	1.5	15	6.99×10^9
9	2	2	1.5	25	6.95×10^9
10	2	2	2.0	15	6.79×10^9
11	2	2	2.0	15	6.92×10^9
12	2	1	1.0	20	7.65×10^9
13	2	1	1.5	15	7.49×10^9
Average					7.36×10^9

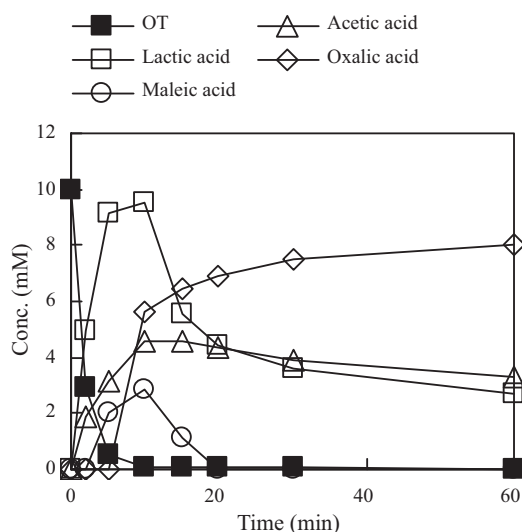


Fig. 6. Carboxylic acids formed during the oxidation of OT by the homogeneous Fenton reaction with 5 mM Fe^{2+} and 200 mM H_2O_2 at pH 3 and 25 °C in a batch reactor.

from the homogeneous Fenton reactor under various conditions, which ranged from 6.79×10^9 to $7.83 \times 10^9 \text{ M}^{-1} \text{ s}^{-1}$ with an average of $7.36 \times 10^9 \text{ M}^{-1} \text{ s}^{-1}$.

3.3.3. Oxidation mechanism determination

To raise the intermediate concentrations to a detectable level, the concentrations of OT, Fe^{2+} , and H_2O_2 were increased to 10, 5, and 200 mM, respectively, and the experiment was conducted in batch mode without AN or solid media. The identified aromatic intermediates were *o*-cresol and 2-nitrotoluene, which had retention times of 4.68 and 5.36 min, respectively, under the selected operating conditions of the gas chromatograph. The match quality was 91% or better in all cases. These results are very similar to OH^\bullet oxidation of 2,6-DMA, in which the methyl group on the benzene ring was more difficult to remove than the amine group [8]. As a result, OH^\bullet reacts preferentially at the amine group through mechanisms similar to those of aniline, as proposed by Brillas et al. [13], Sauleda and Brillas [14], and Oliviero et al. [15]. Several carboxylic acids including acetic, oxalic, lactic, and maleic acids were also identified using the ion chromatograph. The proposed pathway of OT oxidation by OH^\bullet is shown in Fig. 5. The concentration profiles are shown in Fig. 6 and indicate that the aromatic intermediates are rapidly disrupted to form volatile fatty acids while oxalic acid accumulated in the solution. Thus, complete mineralization of OT could not be achieved under the studied conditions.

4. Conclusions

The presence of SiO_2 particles in the complete-mix heterogeneous system did not interfere with the accuracy of the competitive kinetics technique, i.e., the rate constants between OH^\bullet and 2,6-DMA were comparable regardless of the presence of SiO_2 . Additionally, the operating mode (complete-mix versus fluidized-bed)

did not have any significant effect on the rate constant determination. Under varying conditions in a complete-mix homogeneous system, the intrinsic second-order rate constants of OT with OH^\bullet were found to range from 6.79×10^9 to $7.83 \times 10^9 \text{ M}^{-1} \text{ s}^{-1}$ with an average of $7.36 \times 10^9 \text{ M}^{-1} \text{ s}^{-1}$. The amine group on the benzene ring was more susceptible to OH^\bullet attack than the methyl group, and so *o*-cresol and 2-nitrotoluene formed and were sequentially transformed into several carboxylic acids including acetic, oxalic, lactic, and maleic acids.

Acknowledgements

This research was financially supported by the Thailand Research Fund through the Royal Golden Jubilee Ph.D. Program (Grant No. PHD/0056/2549), the National Center of Excellence for Environmental and Hazardous Waste Management of Thailand, the National Research University Project of Thailand's Office of the Higher Education Commission, and the National Science Council of Taiwan (Grant No. NSC96-2628-E-041-001-MY3).

References

- [1] U.S. Department of Health and Human Services, Hazardous Substances Data Bank (HSDB, online database). National Toxicology Information Program, Bethesda, National Library of Medicine, MD. <<http://toxnet.nlm.nih.gov/cgi-bin/sis/search/f?temp/~kWLmes:1>>, 1997 (accessed March 2010).
- [2] International Agency for Research on Cancer, Monographs on the Evaluation of Carcinogenic Risks to Humans, vol. 57, 1993.
- [3] H. Wellens, Zur biologischen Abbaubarkeit mono- und substituierter benzolderivate, Z. Wass. Abwass. Forsch. 23 (3) (1990) 85–98.
- [4] A. Kromann, T.H. Christensen, Degradability of organic chemicals in a landfill environment studied by in situ and laboratory leachate reactors, Waste Manage. Res. 16 (1998) 437–445.
- [5] W.H. Glaze, J.W. Kang, The chemistry of water treatment processes involving ozone, hydrogen peroxide and ultraviolet radiation, Ozone Sci. Eng. 9 (1987) 335–352.
- [6] B.V. Buxton, C.L. Greenstock, W.P. Helman, A.B. Ross, Critical review of rate constants for reactions of hydrated electrons, hydrogen atoms and hydroxyl radicals ($^{\bullet}\text{OH}/^{\bullet}\text{O}^-$) in aqueous solution, J. Phys. Chem. Ref. Data 17 (1998) 513–886.
- [7] J.M. Shen, Z.L. Chen, Z.Z. Xu, Z.Y. Li, B.B. Xu, F. Qi, Kinetics and mechanism of degradation of *p*-chloronitrobenzene in water by ozonation, J. Hazard. Mater. 152 (2008) 1325–1331.
- [8] N. Boonrattanakij, M.C. Lu, J. Anotai, Kinetics and mechanism of 2,6-dimethylaniline degradation by hydroxyl radicals, J. Hazard. Mater. 172 (2009) 952–957.
- [9] NTP, National Toxicology Program, Toxicology and carcinogenesis studies of 2,6-xylydine (2,6-dimethylaniline) in Charles River CD rats (feed studies), TR 278 U.S. Department of Health and Human Services, Public Health Service. <http://ntp.niehs.nih.gov/ntp/htdocs/lt_rpts/tr278.pdf>, 1990 (accessed April 2009).
- [10] J. Anotai, P. Sakulkittimasak, N. Boonrattanakij, M.C. Lu, Kinetics of nitrobenzene oxidation and iron crystallization in fluidized-bed Fenton process, J. Hazard. Mater. 165 (2009) 874–880.
- [11] APHA, Standard Methods for the Examination of Water and Wastewater, 18th edition, American Public Health Association, Washington, DC, 1992.
- [12] I.M. Kolthof, E.B. Sandell, E.J. Meehan, S. Buckstein, Quantitative Chemical Analysis, 4th edition, Macmillan, New York, 1969, pp. 1862–1867.
- [13] E. Brillas, E. Mur, R. Sauleda, L. Sanchez, J. Peral, X. Domenech, J. Casadi, Aniline mineralization by AOP's: anodic oxidation, photocatalysis, electro-Fenton and photoelectro-Fenton processes, Appl. Catal. B: Environ. 16 (1) (1998) 31–42.
- [14] R. Sauleda, E. Brillas, Mineralization of aniline and 4-chlorophenol in acidic solution by ozonation catalyzed with Fe^{2+} and UVA light, Appl. Catal. B: Environ. 29 (2) (2001) 135–145.
- [15] L. Oliviero, H. Wahyu, J. Barbier Jr., D. Duprez, J.W. Ponton, I.S. Metcalfe, D. Mantzavinos, Experimental and predictive approach for determining wet air oxidation reaction pathways in synthetic wastewaters, Chem. Eng. Res. Des. 81 (3) (2003) 384–392.